Nat Commun. Author manuscript; available in PMC 2015 December 24.

Published in final edited form as:
Nat Commun. ; 6: 7479. doi:10.1038/ncomms8479.

Glycan clustering stabilizes the mannose patch of HIV-1 and preserves vulnerability to broadly neutralizing antibodies

Laura K. Pritchard[1], **Daniel I. R. Spencer**[2], **Louise Royle**[2], **Camille Bonomelli**[1], **Gemma E. Seabright**[1], **Anna-Janina Behrens**[1], **Dan Kulp**[3,4], **Sergey Menis**[3,4], **Stefanie A. Krumm**[5], **D. Cameron Dunlop**[1], **Daniel J. Crispin**[1], **Thomas A. Bowden**[6], **Christopher N. Scanlan**[1], **Andrew B. Ward**[7], **William R. Schief**[3,4,8], **Katie J. Doores**[5,*], and **Max Crispin**[1,*]

[1]Oxford Glycobiology Institute, Department of Biochemistry, University of Oxford, South Parks Road, Oxford OX1 3QU, UK

[2]Ludger Ltd., Culham Science Centre, Abingdon, Oxfordshire OX14 3EB, United Kingdom

[3]Department of Immunology and Microbial Science and IAVI Neutralizing Antibody Center, The Scripps Research Institute, La Jolla, CA 92037, USA

[4]Center for HIV/AIDS Vaccine Immunology and Immunogen Discovery, The Scripps Research Institute, La Jolla, CA 92037, USA

[5]King's College London School of Medicine at Guy's, King's and St Thomas' Hospitals, Guy's Hospital, Great Maze Pond, London SE1 9RT, UK

[6]Division of Structural Biology, Wellcome Trust Centre for Human Genetics, University of Oxford, Roosevelt Drive, Oxford OX3 7BN, UK

[7]Department of Integrative Structural and Computational Biology, IAVI Neutralizing Antibody Center, Center for HIV/AIDS Vaccine Immunology and Immunogen Discovery, Skaggs Institute for Chemical Biology, The Scripps Research Institute, 10550 North Torrey Pines Road, La Jolla, CA 92037, USA

[8]Ragon Institute of MGH, MIT and Harvard, Cambridge, MA 02139, USA

Abstract

The envelope spike of HIV-1 employs a 'glycan shield' to protect itself from antibody-mediated neutralization. Paradoxically, however, potent broadly neutralizing antibodies (bnAbs) have been isolated which target this shield. The unusually high glycan density on the gp120 subunit limits processing during biosynthesis, leaving a region of under-processed oligomannose-type structures

*To whom correspondence should be addressed, Max Crispin, max.crispin@bioch.ox.ac.uk, Tel: +44 (0)1865 275381. Katie Doores, katie.doores@kcl.ac.uk, Tel: +44 (0)207 188 3058 .

Author contributions

L.K.P., D.I.R.S., C.B., G.E.S., A.J.B., D.K., S.M., S.A.K. and K.J.D. performed experimental work. L.K.P., D.I.R.S., L.R., A.J.B., D.K., S.M., S.A.K., D.C.D., D.J.C., A.B.W., W.R.S., K.J.D. and M.C. analyzed data. L.K.P., T.A.B., A.B.W., W.R.S., K.J.D. and M.C. wrote the paper. C.N.S., K.J.D. and M.C. designed the study. All authors read and approved the final manuscript.

Competing financial interests

D.I.R.S. and L.R. are employees of Ludger Ltd. The remaining authors declare no competing financial interests.

Europe PMC Funders Author Manuscripts

which is a primary target of these bnAbs. Here we investigate the contribution of individual glycosylation sites to formation of this so-called intrinsic mannose patch. Deletion of individual sites has a limited effect on the overall size of the intrinsic mannose patch but leads to changes in the processing of neighboring glycans. These structural changes are largely tolerated by a panel of glycan-dependent bnAbs targeting these regions, indicating a degree of plasticity in their recognition. These results support the intrinsic mannose patch as a stable target for vaccine design.

Keywords

HIV; N-linked glycosylation; oligomannose; broadly neutralizing antibodies

Introduction

The envelope spike of HIV-1 (Env) orchestrates host cell entry and is the primary target for neutralizing antibodies. Env is a heavily glycosylated molecule, with N-linked glycans accounting for approximately half of the mass of gp120 (ref.[1]). These glycans provide essential roles in protein folding and infectivity[2,3] and also act to shield the underlying protein epitopes from recognition by neutralizing antibodies[4]. The N-linked glycans of gp120 are synthesized using the host cell glycosylation machinery. However, characterization of the glycoforms present has identified a significant population of unprocessed oligomannose-type glycans on gp120, termed the intrinsic mannose patch, which are not usually observed at high abundance on secreted mammalian glycoproteins[5-8]. This divergence from host cell glycosylation is thought to derive from the exceptionally high density of glycans on the outer domain of gp120, which restricts access to ER and Golgi α-mannosidases and prevents the subsequent processing reactions that typically lead to synthesis of complex-type glycans[7].

The ‘non-self’ nature of these oligomannose glycans suggests they could represent a potentially immunogenic target, and indeed a number of broadly neutralizing anti-HIV-1 antibodies (bnAbs) have been isolated which incorporate gp120 glycans as part of their epitope[9-12]. 2G12 was the first such antibody to be described, which exploits an unusual domain-exchanged configuration and binds terminal Manα1→2Man residues on the surface of gp120 (ref.[13-15]). More recently, a collection of bnAbs has been described which recognize dual protein-glycan epitopes[9,11,12,16-25]. A number of these, including PGT121, PGT128 and PGT135, have been demonstrated to be dependent on the outer domain glycan at N332, with this site being referred to as a ‘supersite’ of immune vulnerability[9,17,19,26,27]. Comparison of these bnAbs with those targeting alternative epitopes on gp120, including the CD4-binding site (CD4bs) or membrane-proximal external region (MPER) reveal that they offer some of the highest potencies of neutralization[9]. Furthermore, the different bnAbs derive from various combinations of antibody germline genes, indicating that there are multiple solutions for targeting this region[9,20,28].

Passive transfer of such bnAbs confers resistance to viral challenge in macaque studies[29-31], and thus efforts are being focused to elucidate their precise epitopes, with the aim of designing immunogens capable of eliciting such neutralizing responses through

Europe PMC Funders Author Manuscripts

vaccination[32]. However, a concern regarding the targeting of gp120 glycans relates to the shifting nature of the glycan shield, with additions and deletions of glycan sites being a common response by HIV-1 to antibody-mediated selection pressure[33,34]. Here we investigate the integrity and robustness of the oligomannose population of gp120 in the face of sequence variation, and determine the consequences of glycan site mutation on the formation of bnAb epitopes. Systematic site-directed mutagenesis of the potential N-glycosylation sites (PNGSs) of $gp120_{BaL}$, demonstrates widespread conservation of the oligomannose population, although unexpectedly large perturbations are observed upon loss of certain PNGSs. Structural modeling of the glycan shield reveals protein–glycan and glycan–glycan packing that suggests an explanation for these observations and rationalizes the characteristic processing observed at different glycosylation sites. While it is demonstrated that mutation of sites involved in glycan clusters can lead to subtle 'bystander' processing effects, these changes can largely be tolerated by a panel of bnAbs. The conservation and persistence of oligomannose-type glycans, despite glycan site deletion, suggests that the intrinsic mannose patch is likely to be an important component of an effective vaccine.

Results

Resilience of the mannose patch to glycan site deletion

Site-specific glycosylation analysis of recombinant gp120 indicates that, depending on the isolate, up to half of the PNGSs are occupied by oligomannose-type glycans[1,5,6,35-37]. Given the perceived role of glycan density in driving the formation of the intrinsic mannose patch, it is conceivable that the loss of a single glycan could have a widespread effect on many near and distant glycans by changing the processing state of its neighbors. In this scenario, glycans that would otherwise be protected by a neighboring glycan become exposed and are processed by cellular enzymes to complex-type structures. We therefore sought to investigate the role of an individual glycan site in the formation of the intrinsic mannose patch by site-directed mutagenesis of all 23 gp120 PNGSs of the clade B isolate, BaL.

Asparagine residues within the consensus sequence Asn-X-Ser/Thr (where X is any amino acid except Pro) were mutated to alanine. The gp120 constructs were then expressed transiently in 293T cells and purified by nickel affinity chromatography. Expression of the panel of $gp120_{BaL}$ mutants was performed in parallel to minimize the intrinsic variation of glycosylation (Supplementary Fig. 1; Supplementary Table 1). Following resolution by SDS-PAGE, N-linked glycans were released from monomeric gp120 by treatment with protein *N*-glycosidase F (PNGase F) and analyzed by hydrophilic interaction liquid chromatography-ultra performance liquid chromatography (HILIC-UPLC). HILIC-UPLC was used as it offers a quantitative method for analysis of complex glycan mixtures that is not biased by the glycan composition. Integration of the HILIC-UPLC spectra together with digestions of the fluorescently labeled glycan pool with Endo H enabled the quantitation of oligomannose species.

The HILIC-UPLC chromatogram of the glycans from wild-type $gp120_{BaL}$ reveals a mixture of complex- and oligomannose-type glycans (Fig. 1a). Many of the glycosylation sites on $gp120_{BaL}$ predicted to be of the oligomannose-type[1,35,37,38] (Fig. 1b) show a high degree of

conservation across different clades (Fig. 1c). Changes in the total abundance of oligomannose-type glycans (relative to wild type) were calculated from the HILIC-UPLC data (Fig. 1d; Supplementary Fig. 2; Supplementary Table 2). Overall, the direction of change corresponded well with the predicted glycan species at each site; loss of predicted complex sites showed an increased relative abundance of oligomannose-type glycans, while loss of predicted sites of oligomannose generally resulted in lower relative abundances of oligomannose-type glycans. For a few PNGS-deletions, for example N386 and N392, larger than expected losses of oligomannose were observed (14% and 15% decreases, respectively). These PNGSs may represent sites that normally impede the access of α-mannosidases to neighboring sites, whereby their removal facilitates greater access and trimming of surrounding glycans.

Thus while some mutations lead to larger than expected losses in oligomannose, the majority of PNGS-deletions had a very limited impact on the size of the mannose patch. Several double PNGS-deletion mutants were also analyzed. No dramatic decreases in the overall abundance of oligomannose were observed, with the N295A/N386A double mutant showing the largest effect with a loss of 27% (Fig. 1d; Supplementary Table 2). Since the BaL isolate lacks the N160 and N276 glycans, which are highly conserved and have been shown to be important for recognition by several bnAbs[9,16,39], we also assessed the impact of these glycans by introducing them into the wild-type BaL sequence. These glycans were found to have a limited impact on the size of the mannose patch, either individually or when combined (Supplementary Table 2). Overall these data demonstrate the stability of the size of the mannose patch in the face of glycan site deletion.

Glycan-glycan interactions restrict glycan processing

While the overall size of the mannose patch remained relatively unperturbed upon deletion of individual PNGSs, closer inspection of the HILIC-UPLC traces revealed that the abundances of the individual oligomannose species ($Man_{5\text{-}9}GlcNAc_2$) varied more considerably. Figure 1d shows the change in levels of $Man_9GlcNAc_2$, which displayed the greatest sensitivity to removal of PNGSs (Fig. 1d; Supplementary Table 2). A decrease of over 25% was observed for 9 sites: N130, N262, N295, N339, N356, N386, N392 and N448. These contrasting effects on the overall abundance of oligomannose and $Man_9GlcNAc_2$ alone can be reconciled by the changing proportions of the other oligomannose species. For example at the N295 site no change in the overall level of oligomannose was detectable, however a large decrease in $Man_9GlcNAc_2$ was apparent. This decrease in $Man_9GlcNAc_2$ was offset by an increase in $Man_{6\text{-}8}GlcNAc_2$, suggesting a redistribution of oligomannose species across the intrinsic mannose patch that goes beyond a simple loss of glycans from the N295 site.

The apparent redistribution of glycoforms upon PNGS-deletion, from larger oligomannose-type glycans to smaller oligomannose species, indicates that individual PNGSs have a role in influencing the processing of glycans at neighboring sites. To understand this phenomenon at the structural level, a model of a fully glycosylated $gp120_{BaL}$ trimer was constructed based on the crystal structure of a BG505 SOSIP.664 gp140 trimer[21] (Fig. 2a). $Man_8GlcNAc_2$ glycans were incorporated at sites of predicted oligomannose-type glycans,

while $Man_5GlcNAc_2$ was chosen as a representative mid-sized glycan that is commonly found alongside complex-type glycans at gp120 glycosylation sites (Supplementary Fig. 3). The glycosylated model demonstrates the uniquely high density of glycans on the surface of Env that represents a significant barrier to processing by glycosidases and glycosyltransferases.

Plotting of the changes in $Man_9GlcNAc_2$ abundance on to the gp120 monomer defined a region of high glycan density that was sensitive to deletion of local PNGSs (Fig. 2b). This region mapped to the outer domain of gp120 and is consistent with previous observations of the intrinsic mannose patch[1,5,6,35-37]. Closer inspection of individual PNGSs within this region revealed sites of glycan clusters with two or more glycans positioned in very close proximity. For example one such cluster involves the N386 and N392 glycans, in which the Asn Cα atoms are positioned approximately 12 Å apart. Deletion of the N392 glycan led to an overall decrease in oligomannose abundance of 15% (Fig. 1d and Supplementary Table 2), primarily driven by losses of $Man_9GlcNAc_2$ and $Man_8GlcNAc_2$ (32% and 22% relative to wild-type, respectively; Fig. 2c). Another cluster was identified based around the N295 glycan, which occupies a central location between the N332 and N448 sites. While loss of the N295 glycan had no overall effect on the total abundance of oligomannose, it resulted in a 28% decrease in $Man_9GlcNAc_2$ (Fig. 2c; Supplementary Table 2).

Glycan–glycan interactions within these tight clusters not only suggest an explanation for the limited processing of these glycans, but could rationalize the more widespread changes to glycan processing observed upon removal of a single glycan. It is likely that removal of a glycan within such a cluster increases mobility and accessibility to its neighboring glycan(s), thereby increasing the level of processing that can occur.

Changes in protein conformation distort glycan processing

While many of the PNGS-deletion mutants displayed modest changes in glycosylation, some displayed larger than expected differences that could not be rationalized by cluster effects. One explanation is that either the Asn→Ala mutation, or loss of the glycan, induces protein misfolding, leading to altered glycan processing. To test this possibility ELISAs were performed using b12, a CD4bs conformation-dependent antibody (Fig. 3; Supplementary Table 3). The binding of the majority of the PNGS-mutants was unchanged relative to wild-type, with the exception of N262A and N386A, which displayed significantly reduced binding plateaus. The N262A mutation in particular showed a dramatic change in glycan processing, and this effect was replicated when the N262 site was deleted across a small cross-clade panel (Supplementary Table 4). Reduced binding was also seen for the N262A and N386A mutants with a second conformation-dependent antibody, 17b, which additionally lost binding to the N130A mutant (Fig. 3), presumably through alterations to the structure of the V1 loop[20,40]. These three mutants displayed greater levels of aggregation by Western blotting (Supplementary Fig. 4), supporting the hypothesis that they exhibit a degree of misfolding.

Misfolding of the N130A, N262A and N386A mutants could explain the disproportionately large changes observed in their glycan processing (Fig. 1d). In contrast the significant changes observed for the N295, N339, N356, N392 and N448 mutants are likely to arise

from disruption of glycan clusters leading to improved accessibility by ER and Golgi α-mannosidases.

Effect of PNGS mutation of the N332 site of vulnerability

A number of bnAbs have been isolated which incorporate the N332 glycan as part of their epitope. This so-called 'supersite' of immune vulnerability occupies a central location in the outer domain and lies within a high density of glycans (Fig. 4 and 5a)[20]. Previous studies have indicated this site is occupied by oligomannose-type glycans[1,5,6], suggesting that steric constraints restrict glycan processing at this site. To understand these steric constraints, we studied the location of the N332 glycan on the high-resolution BG505 SOSIP.664 trimer structure[21] and modelled how it would appear to α1,2-mannosidase, the enzyme that initiates glycan processing (Fig. 4). The analysis was based on the glycan conformation of position N332 as revealed by the PGT128 co-crystal structure[17]. This revealed that the high density of glycans clustered around N332 provide significant steric constraints that impede access to the terminal mannose residues of N332 by α1,2-mannosidase. In addition to the constraints created by neighboring glycans, the variable V1 and V4 loops, which project away from the trimer surface, may constitute additional obstacles (Fig. 4c-e).

The high density of glycans in this region raises the question of what effect loss of nearby glycans could have on the processing of the N332 glycan and, importantly, how this may affect recognition by bnAbs. To address this, a tryptic glycopeptide containing the N332 site (QAHCNLSR) was isolated by reverse-phase high performance liquid chromatography (RP-HPLC) fractionation and analyzed by matrix-assisted laser desorption/ionization-mass spectrometry (MALDI-MS) to determine the glycoforms present. The MALDI MS/MS spectrum of the glycopeptide is shown in Supplementary Fig. 5a. Consistent with its structurally constrained location and previous studies, the glycan structures identified at this site were found to be exclusively $Man_8GlcNAc_2$ and $Man_9GlcNAc_2$, with 35% and 65% abundances, respectively (Fig. 5b,c). No smaller oligomannose structures or complex-type glycans were detected. The reproducibility of this method is demonstrated in Supplementary Fig. 5b. To determine if nearby sites played a role in determining the glycan structures present at N332, the same tryptic glycopeptide was purified and analyzed from the N301A, N295A, N339A, N392A and N448A mutants. The MALDI mass spectra of these profiles demonstrated an altered distribution of glycoforms, with $Man_9GlcNAc_2$ being lost in favor of $Man_8GlcNAc_2$ (Fig. 5b,c). In line with its close proximity to N332, loss of the N295 glycan was found to have the largest impact on processing at the N332 site, resulting in an almost complete conversion of $Man_9GlcNAc_2$ to $Man_8GlcNAc_2$. Loss of the N301 glycan, which reaches over the gp120 surface towards N332, also caused a distinct loss of $Man_9GlcNAc_2$ at the N332 site, and smaller changes were also observed for the N339A and N392A mutants. It is likely that the influence of the N448 glycan is mediated through the N295 glycan with which it is clustered.

These observations demonstrate that the environment of a glycan is important in modulating its level of processing. However, at least for the N332 site, the density of surrounding glycans is sufficiently high to act as a buffer for single PNGS-deletions, limiting the effect on processing to minor re-distributions in oligomannose-type structures.

To determine if changes to the glycan shield observed upon glycosylation site deletion could affect antibody recognition, the panel of $gp120_{BaL}$ PNGS-mutants was screened for binding to the N332-dependent bnAbs: 2G12, PGT121, PGT128 and PGT135 (Fig. 6; Supplementary Table 3 gives the IC_{50} values). Consistent with previous reports[13,15,41,42], 2G12 binding was reduced in the N332A, N295A, N386A and N392A mutants. The loss of N295 and N392 were found to be most detrimental to binding, and these glycans have been shown in a 2G12 Fab_2 complex with HIV Env to bind within the conventional V_H/V_L binding site[42]. Interestingly, the effect of the N332-knockout was very modest, and this glycan was shown to bind within the novel secondary V_H/V_H' interface formed by domain exchange in the complex. The loss of N332 was tolerated less well by the PGT antibodies with deletion of known secondary sites also causing reduced binding. Binding by PGT121, which recognizes both oligomannose- and complex- type glycans[19,26], was robust across the remaining panel of mutants with the exception of N262A and N130A which, as discussed above, is a likely consequence of altered protein conformation. Interestingly, the observation that N386A mutation retained binding to PGT121 indicates that perturbations in folding may be localized. In contrast, PGT128 binding appeared to be modestly reduced upon loss of the N295, N386 and N392 sites, which were not contacted by PGT128 in the crystal structure of the antibody-eODmV3 complex[17]. Glycan array data, and the extensive contacts made by PGT128 with the terminal mannose residues of the D1 and D3 arms, support a preferred specificity for $Man_8GlcNAc_2$ and $Man_9GlcNAc_2$ glycans. The decrease in PGT128 binding upon mutation of the N295, N386 and N392 sites may be due to changes in glycan processing or flexibility at the N332/N301 epitope. The observation that N295A retains $Man_8GlcNAc_2$ glycans at N332 (Fig. 5) suggests a role for changes in glycan flexibility for this mutant or altered processing at N301.

Binding of PGT135 was significantly reduced in the N332A and N392A mutants, consistent with their observed roles in antibody binding[20]. Loss of the N295 site, which has been found to be important in a strain-dependent manner, was tolerated in $gp120_{BaL}$, although loss of N386 slightly decreased binding. Additionally, the N339 glycan was also implicated in formation of the PGT135 epitope, either directly or indirectly (Fig. 6). Glycan array data for PGT135, and neutralization of pseudovirus with altered glycosylation profiles, suggests that there is a preference for $Man_7GlcNAc_2$ and $Man_8GlcNAc_2$ glycans at certain sites. Therefore removal of bystander glycan sites that impact the oligomannose structures within the PGT135 epitope could impact binding[20].

Overall, these results show that processing of gp120 glycans are influenced by their environment, with removal of neighboring sites influencing the abundance of different glycan structures present. Such bystander effects were observed at the N332 site, which could explain the dependence of some bnAbs on additional glycan sites not thought to be directly contacted by bnAbs.

Effect of PNGS deletion on virus neutralization

To test the impact of glycan site removal on glycan processing in the context of the HIV-1 envelope trimer, we made several BaL pseudoviruses, each with a single PNGS removed (N130, N262, N295, N301, N332, N386 and N392). The impact of these glycan deletions on

neutralization by our panel of N332-dependent bnAbs and b12 was then analyzed (Fig. 7). Neutralization by b12 was unaffected for the N130A, N295A, N332A, and N392A mutants. However, the N301A and N386A mutants displayed increased sensitivity, consistent with previous observations that removal of these glycans exposes the CD4bs[3]. An increased sensitivity was also observed for the N262A mutant, which could similarly arise from local changes in protein conformation increasing accessibility to the CD4bs. The N262A mutant was also more sensitive to several of the N332-dependent bnAbs, indicating increased accessibility of these epitopes. The effects of the N130A mutation on neutralization were subtler than observed for the gp120 monomer binding, possibly reflecting differences in the assays or, conceivably, the differences in the presentation of that site between monomeric gp120 and virion-associated gp120. However, reduced plateaus were observed for PGT128 and PGT130, which could be a consequence of either altered epitope conformation or glycosylation composition.

Loss of glycan sites known to form bnAb epitopes resulted in reduced neutralization (e.g. N332A for PGT128 and 2G12, N301A for PGT128 and PGT130, N295A for 2G12, N386A for 2G12 and PGT135, and N392A for 2G12 and PGT135). The N332A mutation had a more limited impact on neutralization by PGT130 and PGT121, arising from the ability of these bnAbs to bind adaptably to the mannose patch and utilize alternative glycans in the absence of the N332 glycan[30]. Interestingly bnAbs PGT128, PGT130 and PGT135 were unable to neutralize the wild-type virus to 100%, which could indicate the presence of glycoforms that they are unable to bind. In contrast, PGT121, which has been shown to recognize both complex- and oligomannose-type glycans[19,26], was able to neutralize 100% of the wild-type virus. The N295A mutation was tolerated to varying degrees by the bnAbs, and broadly correlated with the results of the gp120 monomer; neutralization by PGT121 and PGT135 was maintained, while reduced plateaus were observed for PGT128 and PGT130.

Discussion

With the emergence of a large number of glycan-reactive bnAbs, it has become apparent that the ‘non-self’ oligomannose patch within gp120 represents an immunogenic region that could be exploited for vaccine design[32]. This study has demonstrated the persistence of the oligomannose population in the face of glycan-site deletion which, given the shifting nature of the HIV-1 glycan shield[33,34], is an important requirement for ensuring the breadth and potency of a bnAb response. The minimal disruption to processing observed upon deletion of PNGSs suggests that the density of glycans on gp120 is sufficiently high to tolerate individual losses. However it remains to be determined whether there is a critical number of deletions that would reduce the density sufficiently to trigger a larger scale conversion of oligomannose-type glycans to complex-type glycans, and whether or not this is a realistic prospect in native virus given that many sites bearing oligomannose glycans are highly conserved (Fig. 1b and 1c). It is possible that this answer may vary between different isolates, depending on their base level of glycan density.

It is also important to note that additional glycan–glycan and glycan–protein interactions exist within the context of the trimer. By using monomeric gp120 we have focused our study

on the integrity of the intrinsic mannose patch of the outer domain. Given the structural similarity of the outer domain in the context of monomer and trimer, and the conservation of the epitopes of many glycan-dependent antibodies, we suggest that there are also shared rules governing the formation of the intrinsic-mannose patch in monomers and trimers. Although the precise structural factors shaping the formation and stability of trimer glycosylation requires investigation[7,8], we predict that trimerization will only serve to further stabilize glycan processing.

A number of the best characterized glycan-binding bnAbs to date have been found to specifically target the N332 glycan[9,17,19-21], although it is now believed that the area of vulnerability extends across Env[11,12,16,24,25,43]. However, N332 is central to the intrinsic mannose patch and we therefore focused our analysis of PNGS-deletions on the processing of glycoforms at the N332 site, and the consequences for bnAb binding and neutralization. The removal of a single glycan site was found to have a very modest effect on the glycan structures at the N332 site, and this was reflected in the apparent tolerance of a panel of N332-dependent bnAbs to these mutations. The glycan at the N295 site which, when deleted, had the biggest impact on N332 glycan-processing, was an exception. The reduced neutralization displayed by PGT128 and PGT130, which do not directly recognize the N295 glycan, most likely reflects a more widespread perturbation in glycan processing to structures exhibiting reduced antibody binding.

These results provide several important considerations for vaccine design. Firstly, a question that remains to be answered relates to whether a successful immunogen should contain epitopes bearing a more restricted population of glycan structures, in order to generate the most potent response possible, or whether the presence of a more diverse selection of glycoforms would promote a polyclonal response that offers increased breadth. A better understanding of the glycan specificity of bnAbs would help to address this question, as well as site-specific glycan analysis of the functional envelope spike. Secondary to this, it is important to consider how to generate the desired glycoforms on a site-specific basis. Data presented here suggest that in order to reproduce the target epitopes in an immunogen context, it will be necessary to consider the wider environment of the key glycan sites, particularly for oligomannose sites that depend upon a high density of glycans to restrict glycan processing. This study has highlighted important regions of glycan–glycan packing that contribute to maintenance of the oligomannose population, and it is likely that their presence will be necessary to reproduce it in an immunogen context. Our results demonstrate that the presence or absence of individual sites can regulate the precise type of oligomannose structures produced. For example, the levels of the $Man_9GlcNAc_2$ were found to be particularly sensitive to PNGS-deletion, and thus with careful immunogen design it may be possible to precisely fine-tune the degree of glycoform heterogeneity at relevant sites.

One site of note that could emerge as a site of vulnerability is N262 which is almost 100% conserved (Fig. 1c) and has been shown to be occupied by oligomannose-type glycans[137]. Previous studies involving knockout of this glycan have shown it has an important role for infectivity[10,44-46]. While our BaL N262A pseudovirus was still infectious, increased sensitivity to b12 neutralization was indicative of an altered protein conformation, which

was supported by observations of the recombinant N262A $gp120_{BaL}$. In the crystal structure of the BG505 SOSIP.664 trimer[21], the N262 glycan makes extensive contacts with the protein backbone, rationalizing both its protection from endoglycosidase cleavage and its occupation by oligomannose-type glycans. Such a stabilizing role was also observed in a more recent structure of fully-glycosylated gp120 monomer[47]. Oligomannose-type glycans have previously been reported in sites that are inaccessible to glycosidases[48,49], and under-processed glycans often contribute to protein fold stability[50]. The requirement of this glycan is also highlighted by studies with antiviral carbohydrate-binding agents such as cyanovirin-N and Griffithsin, which target oligomannose-type glycans. Resistance profiling with these agents consistently selects for PNGS-deletion mutants, which mostly map to sites known to contain oligomannose glycans including N332, N295, N339, N386, N392 and N448, however deletion of N262 is rarely observed[51-55].

The presence of oligomannose-type glycans on Env has consequences beyond antibody recognition, for example through their interactions with cellular receptors of the immune system. One of the best characterized interactions occurs with the Dendritic Cell-Specific Intercellular adhesion molecule-3 (ICAM)- Grabbing Non-integrin (DC-SIGN) receptor on DCs in the mucosal tissues, which facilitates the trans-infection of $CD4^+$ $CCR5^+$ T cells in secondary lymphoid tissues[56-58]. However more relevant, perhaps, from a vaccine design perspective are observations that oligomannose-type glycans can induce secretion of the immunosuppressive cytokine, IL-10, through interaction with receptors on monocyte-derived DCs[59]. Such an interaction may contribute to the poor immunogenicity of HIV-1 Env as a vaccine candidate, and indeed it has been shown that enzymatic removal of gp120 mannose residues, or occlusion using Griffithsin, improves the immunogenicity of recombinant gp120 (ref.[60,61]). Thus an effective vaccine strategy may have to balance the requirement for faithful replication of bnAb epitopes with the immunogenic properties of vaccine candidates.

In summary, we have shown that the conservation of the oligomannose patch, and its resilience in the face of glycan-site deletion, makes it a robust target for vaccine design. Multiple bnAbs have been isolated which display subtly different, yet overlapping, epitopes within this region, suggesting that the induction of a polyclonal response against it would protect against a diverse viral swarm. Furthermore, data presented here on the persistence of the mannose patch provide important insights for the design of future candidate immunogens.

Methods

Site-directed mutagenesis

The cloning of $gp120_{BaL}$ into the pHLsec expression vector has previously been described[62]. Individual knockout of all 23 PNGSs of BaL gp120 was performed by mutating asparagines (within the sequence Asn-X-Ser/Thr, where X is any amino acid except proline) to alanine. Mutagenesis was performed by the overlap extension PCR method[63], using approximately 1 ng of WT pHLsec.BaL as the template DNA. A list of primers used is given in Supplementary Table 5. The full Env sequence for each construct was verified by DNA sequencing. Mutations in the full-length envelope were made using site-directed

mutagenesis and the sequences were verified by DNA sequencing. A list of primers used is given in Supplementary Table 6.

Protein expression and purification

Human embryonic kidney (HEK) 293T cells were purchased from the American Type Culture Collection and maintained in Dulbecco's Modified Eagle's Medium containing 10% fetal bovine serum, 50 U ml^{-1} penicillin, and 50 μg ml^{-1} streptomycin. Recombinant gp120s were expressed under serum free conditions, by transient transfection of expression plasmids using polyethylenimine (PEI) in a PEI:DNA ratio of 3.5:1 (w/w). Comparable mutants were expressed in parallel to avoid variation arising from fluctuating cell culture conditions. Transfected cultures were incubated for 3 days before supernatants were harvested and filtered through a 0.22 μM membrane (Millipore). Gp120 was purified by immobilized metal affinity chromatography using a HisTrap HP column (GE Healthcare) according to manufacturer's instructions. Eluted fractions were concentrated using 50 kDa cut-off centrifugal spin filters (Vivaspin).

Enzymatic release of N-linked glycans

N-linked glycans were released from gp120 in-gel using PNGase F (New England Biolabs). His-purified gp120 was resolved by SDS-PAGE and stained with Coomassie Blue. Following destaining, the band corresponding to monomeric gp120 was excised and washed extensively with acetonitrile and water. Gel bands were then incubated with PNGase F for 16 hours at 37°C, following manufacturer's instructions. Released glycans were eluted from the gel with water and dried in a SpeedVac concentrator.

Fluorescent labelling of N-linked glycans

Released glycans were subsequently fluorescently labelled and purified as previously described[64]. Briefly, dried glycans were resuspended in 30 μl water before addition of 80 μl labelling mixture (comprising 30 mg ml^{-1} 2-aminobenzoic acid [2-AA] and 45 mg ml^{-1} sodium cyanoborohydride in a solution of sodium acetate trihydrate [4% w/v] and boric acid [2% w/v] in methanol). Samples were incubated at 80°C for 1 h then allowed to cool. Excess label was removed using Spe-ed Amide-2 cartridges.

HILIC-UPLC analysis of N-linked glycans

Fluorescently labelled glycans were separated by HILIC-UPLC using a 2.1 mm × 10 mm Acquity BEH Amide Column (1.7 μm particle size; Waters, Elstree, UK). The following gradient was run: time = 0 min (t=0): 22% A, 78% B (flow rate of 0.5 ml min^{-1}); t= 38.5: 44.1% A, 55.9% B (0.5 ml min^{-1}); t=39.5: 100% A, 0% B (0.25 ml min^{-1}); t=44.5: 100% A, 0% B; t=46.5: 22% A, 78% B (0.5 ml min^{-1}), where solvent A was 50 mM ammonium formate, pH 4.4, and solvent B was acetonitrile. Fluorescence was measured using an excitation wavelength of 330 nm and a detection wavelength of 420 nm. Difference plots were generated in MATLAB (The MathWorks, Inc).

Europe PMC Funders Author Manuscripts

Enzymatic digestion of released glycans

The abundance of oligomannose glycans was measured by digestion with Endoglycosidase H, which cleaves oligomannose-type glycans but not complex-type glycans (Endo H; New England Biolabs). 2-AA labelled glycans were resuspended in water and digested with Endo H for 16 hours at 37°C, according to manufacturer's instructions. Digested glycans were cleaned using a PVDF protein-binding membrane plate prior to HILIC-UPLC analysis. The abundance of oligomannose-type glycans was calculated, as a relative percentage, by integration of the HILIC-UPLC chromatograms before and after Endo H digestion, following normalization. The magnitude of change was calculated as a % change in abundance, relative to wild-type.

Structural modelling of glycosylated Env

A model of the BaL gp120 trimer was constructed using the recently solved atomic-level resolution structure of a BG505 SOSIP.664 gp140 trimer (PDB accession code: 4NCO)[21]. First, atomic clashes present in the 4NCO crystal structure were relieved and missing side-chains rebuilt, by executing 1,000 symmetric ROSETTA-fixbb simulations, selecting the lowest scoring model, and then running a constrained ROSETTA-relax simulation. Next, the BaL sequence was modeled onto the gp120 trimer structure, by running 1,000 ROSETTA-remodel trajectories[65], which included building new conformations for the variable loops, and then filtering the models by structural metrics. The best 15 models were considered as an ensemble of possible BaL gp120 trimer structures, as each model was in the top 33% of the 3 structural metrics Ramachandran (rama), attractive portion of the Lennard-Jones potential (fa_atr) and the total ROSETTA score.

Each N-linked glycosylation motif for each of the 15 models was decorated with $Man_8GlcNAc_2$ glycans at sites of predicted oligomannose-type glycans and with $Man_5GlcNAc_2$ glycans at remaining sites. GlycanRelax[66] was used to approximate the conformational behavior of glycans in a glycoprotein context. For each model, 10 separate GlycanRelax trajectories of 10000 cycles of MonteCarlo trials were carried out. Each glycan on the gp120 was allowed to move independently throughout the GlycanRelax minimization. A single low energy model was chosen for the figures.

Purification of an N332 glycopeptide

Gp120 was resolved by SDS-PAGE, and the monomer excised and washed as described above. Reduction was carried out by addition of 10 mM Dithiothreitol in 100 mM ammonium bicarbonate and incubation at 65°C for 30 mins. Alkylation was subsequently performed by addition of 50 mM Iodoacetamide in 100 mM ammonium bicarbonate, with incubation at room temperature for 50 mins. Trypsin (Promega) was then added at a concentration of 12.5 μg ml^{-1} and incubated at 37°C for 16 hours. Glycopeptides were eluted from the gel with alternate washes of water and acetonitrile, filtered through a 0.45 μM membrane (Whatman), and dried in a SpeedVac concentrator. After resuspension in 0.1% TFA, the glycopeptide pool was fractionated by reverse phase-HPLC using a Jupiter C18 5 μm 250 × 4.5 mm column (300 Å pore size) (Phenomenex) and a Dionex U3000 LC system. The following gradient was run at a flow rate of 1 ml min^{-1}, with fractions being collected every minute for 90 minutes: time = 0 min (t=0): 95% A, 5% B; t= 5: 95% A, 5%

B; *t*=90: 10% A, 90% B; *t*=95: 10% A, 90% B; *t*=97: 95% A, 5% B; *t*= 120: 95% A, 5% B, where solvent A was 50 mM ammonium formate, pH 4.4, and solvent B was acetonitrile. UV absorbance was detected at 214 and 280 nm.

Mass spectrometric analysis of glycopeptides

Glycopeptide fractions were desalted using C18 ZipTip® pipette tips, according to manufacturer's instructions, before spotting onto a ground steel target plate in a solution of 10 mg ml^{-1} 2,5-Dihydrozybenzoic acid in 50% acetonitrile. MALDI-MS was performed using an Autoflex™ Speed MALDI-TOF/TOF instrument (Bruker), operated in positive ion mode. MS/MS was performed to confirm the peptide identity.

ELISA

Antibodies b12, 2G12, PGT121, PGT128 and PGT135 were obtained from the International AIDS Vaccine Initiative (IAVI, New York, NY). Microtitre ELISA plates (Corning) were coated with mouse anti-HIS capture antibody (2 μg mL^{-1} in PBS; Life Technologies) overnight at 4 °C. Plates were washed five times with a solution of PBS containing 0.05% Tween 20 (v/v) and then blocked for 1 h at room temperature with 5% non-fat milk in PBS + 0.05% Tween (blocking buffer). Gp120 was then added at a concentration of 2 μg ml^{-1} in blocking buffer, followed by incubation for 1 h at room temperature. Plates were washed (×5) before addition of primary antibodies (b12, 17b, 2G12, PGT121, PGT128 & PGT135). A 1:5 dilution series was used starting at 20 μg ml^{-1} or 40 μg ml^{-1} in blocking buffer. Incubation was carried out at room temperature for 2 h. Plates were then washed (×5) and alkaline phosphatase-conjugated goat anti-human Fab secondary antibody (Thermo Scientific Pierce) was added as a 1:1000 dilution in blocking buffer. Plates were washed (×5) and then AP substrate (50 μL per well) was added. Once color had developed the OD at 405 nm was measured.

Virus neutralization assay

To produce pseudoviruses, plasmids encoding Env were co-transfected with an Env-deficient genomic backbone plasmid (pSG3ΔEnv) in a 1:2 ratio with the transfection reagent PEI (1 mg mL^{-1}, 1:3 PEI:total DNA, Polysciences) into HEK 293T cells. Pseudoviruses were harvested 72 h post transfection for use in neutralization assays[67]. Neutralizing activity was assessed using a single round replication pseudovirus assay with TZM-bl target cells, as described previously[68]. Briefly, TZM-bl cells were seeded in a 96-well flat bottom plate at a concentration of 20,000 cells per well. The serially diluted antibody/virus mixture, which was pre-incubated for 1 h, was then added to the cells and luminescence was quantified 72 h following infection via lysis and addition of Bright-Glo™ Luciferase substrate (Promega). To determine IC_{50} values, serial dilutions of mAbs were incubated with wild-type virus or mutant virus and the dose-response curves were fitted using nonlinear regression.

Supplementary Material

Refer to Web version on PubMed Central for supplementary material.

Europe PMC Funders Author Manuscripts

Acknowledgements

We would like to dedicate this article in memory of our much valued friend and greatly admired colleague, Dr Chris Scanlan. We thank Dr Li Phing Liew for technical assistance, and Prof. Raymond A. Dwek, Prof. David J. Harvey, Dr Daryl Fernandes and Dr Holger Kramer for support and helpful discussions. L.K.P. has been supported by a Scholarship from the Department of Biochemistry, University of Oxford. M.C. is a Fellow of Oriel College, Oxford. This work was supported by International AIDS Vaccine Initiative Neutralizing Antibody Center and NAC CAVD grant (A.B.W., W.R.S. and M.C.), National Institute of Allergy and Infectious Diseases grants P01AI081625 (W.R.S.), 1UM1AI100663 (CHAVI-ID to M.C., A.B.W. and W.R.S.), the Medical Research Council MR/K024426/1 (K.J.D.) and MR/L009528/1 (T.A.B.), and Wellcome Trust Grant 090532/Z/09/Z (T.A.B.).

References

1. Leonard CK, et al. Assignment of intrachain disulfide bonds and characterization of potential glycosylation sites of the type 1 recombinant human immunodeficiency virus envelope glycoprotein (gp120) expressed in Chinese hamster ovary cells. J. Biol. Chem. 1990; 265:10373–82. [PubMed: 2355006]
2. Li Y, Luo L, Rasool N, Kang CY. Glycosylation is necessary for the correct folding of human immunodeficiency virus gp120 in CD4 binding. J. Virol. 1993; 67:584–8. [PubMed: 8416385]
3. Binley JM, et al. Role of complex carbohydrates in human immunodeficiency virus type 1 infection and resistance to antibody neutralization. J. Virol. 2010; 84:5637–55. [PubMed: 20335257]
4. Reitter JN, Means RE, Desrosiers RC. A role for carbohydrates in immune evasion in AIDS. Nat. Med. 1998; 4:679–684. [PubMed: 9623976]
5. Zhu X, Borchers C, Bienstock RJ, Tomer KB. Mass spectrometric characterization of the glycosylation pattern of HIV-gp120 expressed in CHO cells. Biochemistry. 2000; 39:11194–204. [PubMed: 10985765]
6. Go EP, et al. Glycosylation site-specific analysis of HIV envelope proteins (JR-FL and CON-S) reveals major differences in glycosylation site occupancy, glycoform profiles, and antigenic epitopes' accessibility. J. Proteome Res. 2008; 7:1660–1674. [PubMed: 18330979]
7. Doores KJ, et al. Envelope glycans of immunodeficiency virions are almost entirely oligomannose antigens. Proc. Natl. Acad. Sci. U. S. A. 2010; 107:13800–13805. [PubMed: 20643940]
8. Bonomelli C, et al. The glycan shield of HIV is predominantly oligomannose independently of production system or viral clade. PLoS One. 2011; 6:e23521. [PubMed: 21858152]
9. Walker LM, et al. Broad neutralization coverage of HIV by multiple highly potent antibodies. Nature. 2011; 477:466–70. [PubMed: 21849977]
10. Lavine CL, et al. High-mannose glycan-dependent epitopes are frequently targeted in broad neutralizing antibody responses during human immunodeficiency virus type 1 infection. J. Virol. 2012; 86:2153–64. [PubMed: 22156525]
11. Scharf L, et al. Antibody 8ANC195 reveals a site of broad vulnerability on the HIV-1 envelope spike. Cell Rep. 2014; 7:785–95. [PubMed: 24767986]
12. Huang J, et al. Broad and potent HIV-1 neutralization by a human antibody that binds the gp41–gp120 interface. Nature. 2014; 515:138–142. [PubMed: 25186731]
13. Scanlan CN, et al. The broadly neutralizing anti-human immunodeficiency virus type 1 antibody 2G12 recognizes a cluster of α1→2 mannose residues on the outer face of gp120. J. Virol. 2002; 76:7306–7321. [PubMed: 12072529]
14. Sanders RW, et al. The mannose-dependent epitope for neutralizing antibody 2G12 on human immunodeficiency virus type 1 glycoprotein gp120. J. Virol. 2002; 76:7293–7305. [PubMed: 12072528]
15. Calarese, D. a, et al. Antibody domain exchange is an immunological solution to carbohydrate cluster recognition. Science. 2003; 300:2065–71. [PubMed: 12829775]
16. Walker LM, et al. Broad and potent neutralizing antibodies from an African donor reveal a new HIV-1 vaccine target. Science. 2009; 326:285–9. [PubMed: 19729618]
17. Pejchal R, et al. A potent and broad neutralizing antibody recognizes and penetrates the HIV glycan shield. Science. 2011; 334:1097–103. [PubMed: 21998254]

18. McLellan JS, et al. Structure of HIV-1 gp120 V1/V2 domain with broadly neutralizing antibody PG9. Nature. 2011; 480:336–43. [PubMed: 22113616]
19. Mouquet H, et al. Complex-type N-glycan recognition by potent broadly neutralizing HIV antibodies. Proc. Natl. Acad. Sci. U. S. A. 2012; 109:E3268–77. [PubMed: 23115339]
20. Kong L, et al. Supersite of immune vulnerability on the glycosylated face of HIV-1 envelope glycoprotein gp120. Nat. Struct. Mol. Biol. 2013; 20:796–803. [PubMed: 23708606]
21. Julien J-P, et al. Crystal structure of a soluble cleaved HIV-1 envelope trimer. Science. 2013; 342:1477–83. [PubMed: 24179159]
22. Pancera M, et al. Structural basis for diverse N-glycan recognition by HIV-1-neutralizing V1-V2-directed antibody PG16. Nat. Struct. Mol. Biol. 2013; 20:804–13. [PubMed: 23708607]
23. Julien J-P, et al. Asymmetric recognition of the HIV-1 trimer by broadly neutralizing antibody PG9. Proc. Natl. Acad. Sci. U. S. A. 2013; 110:4351–6. [PubMed: 23426631]
24. Blattner C, et al. Structural delineation of a quaternary, cleavage-dependent epitope at the gp41-gp120 interface on intact HIV-1 Env trimers. Immunity. 2014; 40:669–80. [PubMed: 24768348]
25. Falkowska E, et al. Broadly neutralizing HIV antibodies define a glycan-dependent epitope on the prefusion conformation of gp41 on cleaved envelope trimers. Immunity. 2014; 40:657–68. [PubMed: 24768347]
26. Julien J-P, et al. Broadly neutralizing antibody PGT121 allosterically modulates CD4 binding via recognition of the HIV-1 gp120 V3 base and multiple surrounding glycans. PLoS Pathog. 2013; 9:e1003342. [PubMed: 23658524]
27. Sok D, et al. Promiscuous glycan site recognition by antibodies to the high-mannose patch of gp120 broadens neutralization of HIV. Sci. Transl. Med. 2014; 6:236ra63.
28. Sok D, et al. The effects of somatic hypermutation on neutralization and binding in the PGT121 family of broadly neutralizing HIV antibodies. PLoS Pathog. 2013; 9:e1003754. [PubMed: 24278016]
29. Mascola JR, et al. Protection of macaques against vaginal transmission of a pathogenic HIV-1/SIV chimeric virus by passive infusion of neutralizing antibodies. Nat. Med. 2000; 6:207–10. [PubMed: 10655111]
30. Hessell AJ, et al. Broadly neutralizing human anti-HIV antibody 2G12 is effective in protection against mucosal SHIV challenge even at low serum neutralizing titers. PLoS Pathog. 2009; 5:e1000433. [PubMed: 19436712]
31. Moldt B, et al. Highly potent HIV-specific antibody neutralization in vitro translates into effective protection against mucosal SHIV challenge in vivo. Proc. Natl. Acad. Sci. U. S. A. 2012; 109:18921–5. [PubMed: 23100539]
32. Burton DR, et al. A blueprint for HIV vaccine discovery. Cell Host Microbe. 2012; 12:396–407. [PubMed: 23084910]
33. Wei X, et al. Antibody neutralization and escape by HIV-1. Nature. 2003; 422:307–12. [PubMed: 12646921]
34. Moore PL, et al. Evolution of an HIV glycan – dependent broadly neutralizing antibody epitope through immune escape. Nat. Med. 2012; 18:1688–1692. [PubMed: 23086475]
35. Cutalo JM, Deterding LJ, Tomer KB. Characterization if glycopeptides from HIV-1 SF2 gp120 by liquid chromatography mass spectrometry. J. Am. Soc. Mass Spectrom. 2004; 15:1545–1555. [PubMed: 15519221]
36. Go EP, et al. Glycosylation site-specific analysis of clade C HIV-1 envelope proteins. J. Proteome Res. 2009; 8:4231–4242. [PubMed: 19610667]
37. Pabst M, Chang M, Stadlmann J, Altmann F. Glycan profiles of the 27 N-glycosylation sites of the HIV envelope protein CN54gp140. Biol. Chem. 2012; 393:719–30. [PubMed: 22944675]
38. Go EP, et al. Characterization of host-cell line specific glycosylation profiles of early transmitted/founder HIV-1 gp120 envelope proteins. J. Proteome Res. 2013; 12:1223–34. [PubMed: 23339644]
39. West AP, et al. Computational analysis of anti-HIV-1 antibody neutralization panel data to identify potential functional epitope residues. Proc. Natl. Acad. Sci. U. S. A. 2013; 110:10598–603. [PubMed: 23754383]

40. Kwong PD, et al. Structure of an HIV gp120 envelope glycoprotein in complex with the CD4 receptor and a neutralizing human antibody. Nature. 1998; 393:648–59. [PubMed: 9641677]
41. Trkola A, et al. Human monoclonal antibody 2G12 defines a distinctive neutralization epitope on the gp120 glycoprotein of human immunodeficiency virus type 1. J. Virol. 1996; 70:1100–8. [PubMed: 8551569]
42. Murin CD, et al. Structure of 2G12 Fab2 in complex with soluble and fully glycosylated HIV-1 Env by negative-stain single particle electron microscopy. J. Virol. 2014; 88:10177–10188. [PubMed: 24965454]
43. Chuang G-Y, et al. Residue-level prediction of HIV-1 antibody epitopes based on neutralization of diverse viral strains. J. Virol. 2013; 87:10047–58. [PubMed: 23843642]
44. Willey RL, et al. In vitro mutagenesis identifies a region within the envelope gene of the human immunodeficiency virus that is critical for infectivity. J. Virol. 1988; 62:139–47. [PubMed: 3257102]
45. François KO, Balzarini J. The highly conserved glycan at asparagine 260 of HIV-1 gp120 is indispensable for viral entry. J. Biol. Chem. 2011; 286:42900–10. [PubMed: 22006924]
46. Wang W, et al. A systematic study of the N-glycosylation sites of HIV-1 envelope protein on infectivity and antibody-mediated neutralization. Retrovirology. 2013; 10:14. [PubMed: 23384254]
47. Kong L, Wilson IA, Kwong PD. Crystal structure of a fully glycosylated HIV-1 gp120 core reveals a stabilizing role for the glycan at Asn262. Proteins Struct. Funct. Bioinforma. 2015; 83:590–596.
48. Crispin MDM, et al. Monoglucosylated glycans in the secreted human complement component C3: implications for protein biosynthesis and structure. FEBS Lett. 2004; 566:270–4. [PubMed: 15147907]
49. Crispin M, et al. Structural Plasticity of the Semliki Forest Virus Glycome upon Interspecies Transmission. J. Proteome Res. 2014; 13:1702–1712. [PubMed: 24467287]
50. Gala, F. a; Morrison, SL. The role of constant region carbohydrate in the assembly and secretion of human IgD and IgA1. J. Biol. Chem. 2002; 277:29005–11. [PubMed: 12023968]
51. Balzarini J, et al. Mutational pathways, resistance profile, and side effects of cyanovirin relative to human immunodeficiency virus type 1 strains with N-glycan deletions in their gp120 envelopes. J. Virol. 2006; 80:8411–21. [PubMed: 16912292]
52. Witvrouw M, et al. Resistance of human immunodeficiency virus type 1 to the high-mannose binding agents cyanovirin N and concanavalin A. J. Virol. 2005; 79:7777–7784. [PubMed: 15919930]
53. Hu Q, Mahmood N, Shattock RJ. High-mannose-specific deglycosylation of HIV-1 gp120 induced by resistance to cyanovirin-N and the impact on antibody neutralization. Virology. 2007; 368:145–54. [PubMed: 17658575]
54. Alexandre KB, et al. Mannose-rich glycosylation patterns on HIV-1 subtype C gp120 and sensitivity to the lectins, Griffithsin, Cyanovirin-N and Scytovirin. Virology. 2010; 402:187–96. [PubMed: 20392471]
55. Huang X, Jin W, Griffin GE, Shattock RJ, Hu Q. Removal of two high-mannose N-linked glycans on gp120 renders human immunodeficiency virus 1 largely resistant to the carbohydrate-binding agent griffithsin. J. Gen. Virol. 2011; 92:2367–73. [PubMed: 21715597]
56. Geijtenbeek TB, et al. DC-SIGN, a dendritic cell-specific HIV-1-binding protein that enhances trans-infection of T cells. Cell. 2000; 100:587–97. [PubMed: 10721995]
57. Kwon DS, Gregorio G, Bitton N, Hendrickson W. a, Littman DR. DC-SIGN-mediated internalization of HIV is required for trans-enhancement of T cell infection. Immunity. 2002; 16:135–44. [PubMed: 11825572]
58. Hong PW, et al. Human immunodeficiency virus envelope (gp120) binding to DC-SIGN and primary dendritic cells is carbohydrate dependent but does not involve 2G12 or cyanovirin binding sites: implications for structural analyses of gp120-DC-SIGN binding. J. Virol. 2002; 76:12855–12865. [PubMed: 12438611]
59. Shan M, et al. HIV-1 gp120 mannoses induce immunosuppressive responses from dendritic cells. PLoS Pathog. 2007; 3:e169. [PubMed: 17983270]

60. Banerjee K, et al. Enzymatic removal of mannose moieties can increase the immune response to HIV-1 gp120 in vivo. Virology. 2009; 389:108–21. [PubMed: 19410272]
61. Banerjee K, et al. Occluding the mannose moieties on human immunodeficiency virus type 1 gp120 with griffithsin improves the antibody responses to both proteins in mice. AIDS Res. Hum. Retroviruses. 2012; 28:206–14. [PubMed: 21793733]
62. Dunlop DC, et al. Polysaccharide mimicry of the epitope of the broadly neutralizing anti-HIV antibody, 2G12, induces enhanced antibody responses to self oligomannose glycans. Glycobiology. 2010; 20:812–23. [PubMed: 20181792]
63. Ho SN, Hunt HD, Horton RM, Pullen JK, Pease LR. Site-directed mutagenesis by overlap extension using the polymerase chain reaction. Gene. 1989; 77:51–9. [PubMed: 2744487]
64. Neville DCA, Dwek RA, Butters TD. Development of a single column method for the separation of lipid- and protein-derived oligosaccharides. J. Proteome Res. 2009; 8:681–687. [PubMed: 19099509]
65. Huang P-S, et al. RosettaRemodel: a generalized framework for flexible backbone protein design. PLoS One. 2011; 6:e24109. [PubMed: 21909381]
66. Pancera M, et al. Structure of HIV-1 gp120 with gp41-interactive region reveals layered envelope architecture and basis of conformational mobility. Proc. Natl. Acad. Sci. U. S. A. 2010; 107:1166–71. [PubMed: 20080564]
67. Montefiori DC. Evaluating neutralizing antibodies against HIV, SIV, and SHIV in luciferase reporter gene assays. Curr. Protoc. Immunol. 2005 **Chapter 12,** Unit 12.11.
68. Walker LM, et al. Rapid development of glycan-specific, broad, and potent anti-HIV-1 gp120 neutralizing antibodies in an R5 SIV/HIV chimeric virus infected macaque. Proc. Natl. Acad. Sci. U. S. A. 2011; 108:20125–9. [PubMed: 22123961]
69. Bowden, T. a, et al. Chemical and structural analysis of an antibody folding intermediate trapped during glycan biosynthesis. J. Am. Chem. Soc. 2012; 134:17554–63. [PubMed: 23025485]
70. Harvey DJ, et al. Proposal for a standard system for drawing structural diagrams of N- and O-linked carbohydrates and related compounds. Proteomics. 2009; 9:3796–801. [PubMed: 19670245]

Europe PMC Funders Author Manuscripts

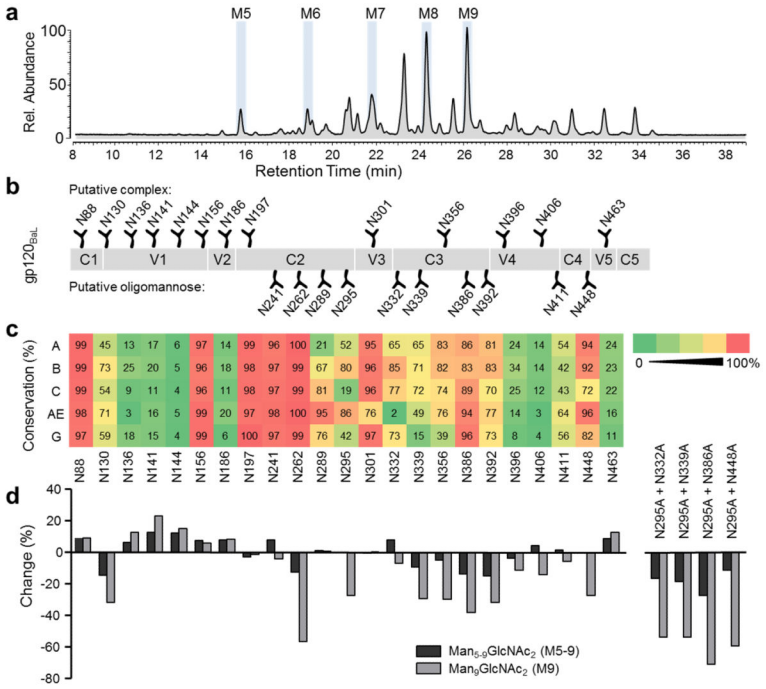

Figure 1. Contribution of individual glycans to the total glycosylation of $gp120_{BaL}$

(**a**) HILIC-UPLC profile of N-linked glycans released from $gp120_{BaL}$. The $Man_{5\text{-}9}GlcNAc_2$ series is labelled M5–M9 and highlighted in blue. Remaining peaks correspond to hybrid and complex-type glycans (**b**) Schematic showing the distribution of the 23 PNGSs of $gp120_{BaL}$. Sites were allocated as putative complex-type or putative oligomannose-type based on previous reports[1,35-37]. (**c**) Percentage conservation of the individual PNGSs across different clades, based on analysis of over 4000 aligned Env sequences from the Los Alamos HIV sequence database (http://www.hiv.lanl.gov/). (**d**) Effect of PNGS-deletion on the total abundance of oligomannose-type glycans, and the individual abundance of $Man_9GlcNAc_2$. Values were obtained by integration of corresponding HILIC-UPLC peaks (Supplementary Fig. 2), before and after Endoglycosidase H treatment, and represent the percentage change in abundance (relative to wild-type). Percentage change = [(% oligomannose in wild-type − % oligomannose in mutant)/(% oligomannose in wild-type)] × 100. Values are reported in Supplementary Table 2. The dashed line represents the predicted drop in oligomannose levels from the elimination of one site containing only oligomannose-type glycans.

Europe PMC Funders Author Manuscripts

Europe PMC Funders Author Manuscripts

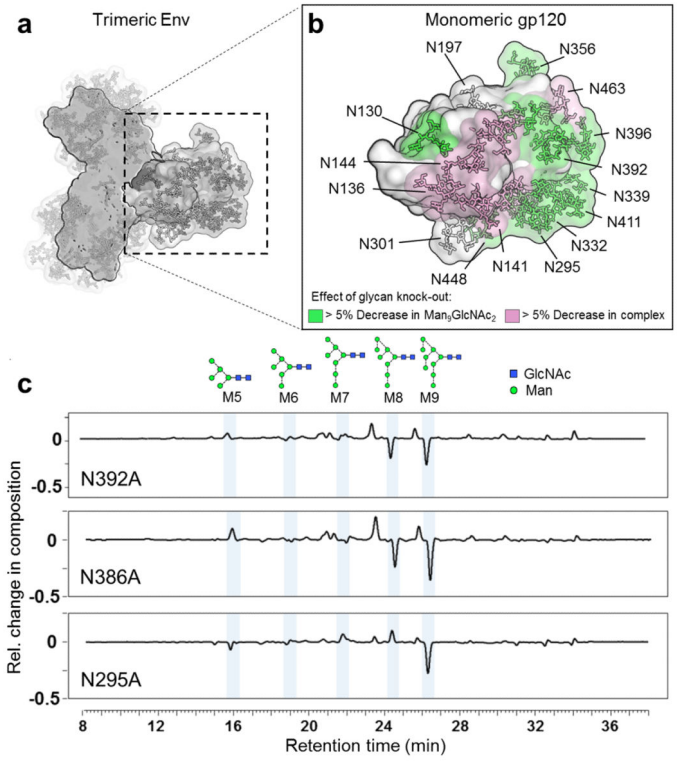

Figure 2. Role of glycan clusters in maintaining the oligomannose population

(**a**) Model of a fully glycosylated BaL trimer based on the reported gp140 trimer crystal structure[21] (PDB accession code: 4NCO). Modelled glycans are shown as sticks. The surface of the glycans and underlying protein are depicted in shades of gray. $Man_5GlcNAc_2$ glycans were modelled at sites of predicted complex-type glycans and $Man_8GlcNAc_2$ glycans were added at predicted oligomannose sites. (**b**) A close-up view of the gp120 monomer. Glycans are colored according to the effect of their elimination on total $Man_9GlcNAc_2$ levels or complex-type glycosylation according to Fig 1d. A change of over 5% is greater than the intrinsic variation of glycosylation (Supplementary Fig. 1; Supplementary Table 1). (**c**) Examples of changes in glycan composition upon deletion of individual glycan sites of the mannose patch. Residual plots were calculated by the subtraction of HILIC-UPLC spectra of PNGS-deletion mutants from that of the wild-type. Peaks corresponding to oligomannose-type glycans are highlighted. $Man_{5\text{-}9}GlcNAc_2$ (M5–9) are schematically labelled according to the combined nomenclature[69] of Harvey *et al*[70] and the Center of Functional Glycomics.

Europe PMC Funders Author Manuscripts

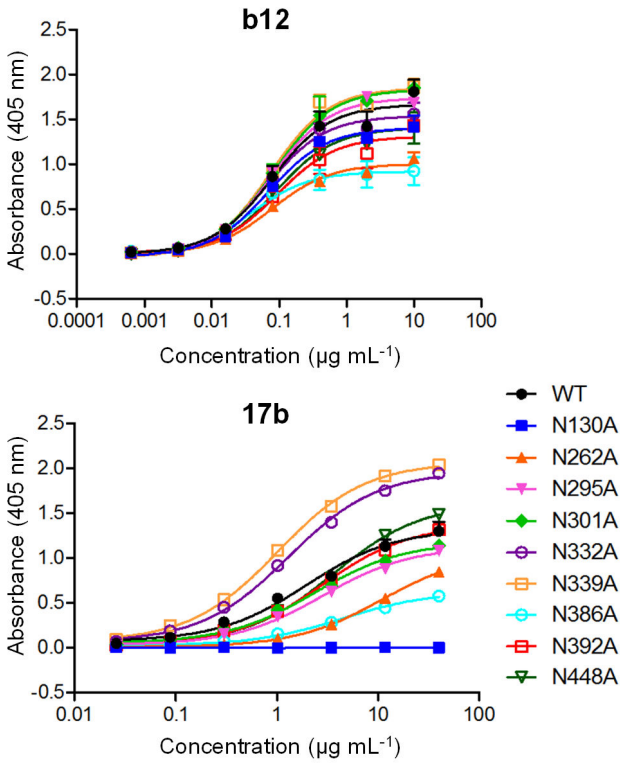

Figure 3. Recognition of PNGS-deletion mutants by conformation-dependent antibodies

Binding of the conformation-dependent monoclonal antibodies b12 and 17b was tested against the panel of $gp120_{BaL}$ PNGS-deletion mutants by capture ELISA. Error bars represent standard deviation. Each experiment was performed in duplicate and repeated three times.

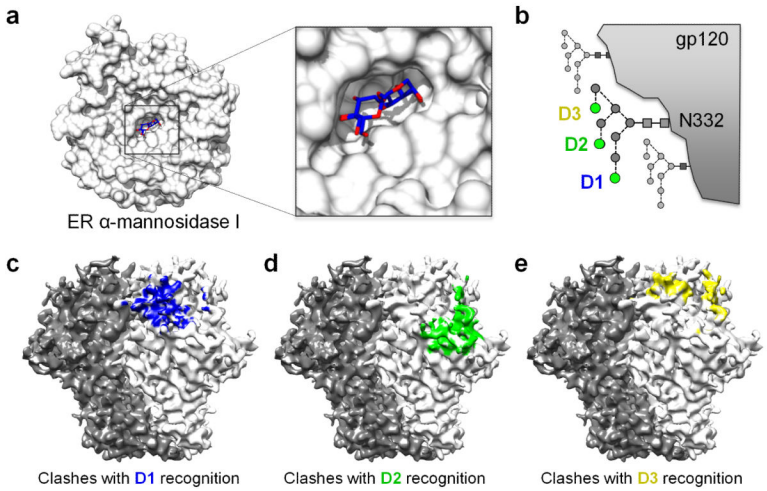

Figure 4. Steric barriers to the processing of Env glycans

The α-mannosidase enzyme has impeded access to the terminal sugars of the mannose patch due to steric constraints imposed by both protein and glycan moieties. (**a**) The high-resolution structure of α1,2-mannosidase (PDB accession code: 2RI9) bound to a disaccharide substrate shows how the substrate binds in a deep, concave pocket. (**b**) When the α-1,2-mannosidase structure is docked onto the surface of the HIV-1 Env trimer (hybrid model of EMD-5779 and PDB 3TYG) and aligned on the terminal D1, D2, or D3 arms of the $Man_9GlcNAc_2$ moiety at position N332, there are significant clashes (**c-e**). In those three panels, the colored surfaces represent areas of the trimer that are within 2 Å of α-1,2-mannosidase after docking the terminal mannoses on $Man_9GlcNAc_2$ into the binding enzyme pocket, i.e., clashes occur that impede enzyme access to its glycan substrates and are therefore predicted to prevent glycan processing. The variable loops V4 and V1 account for a large proportion of the clashes seen in panels d and e, respectively.

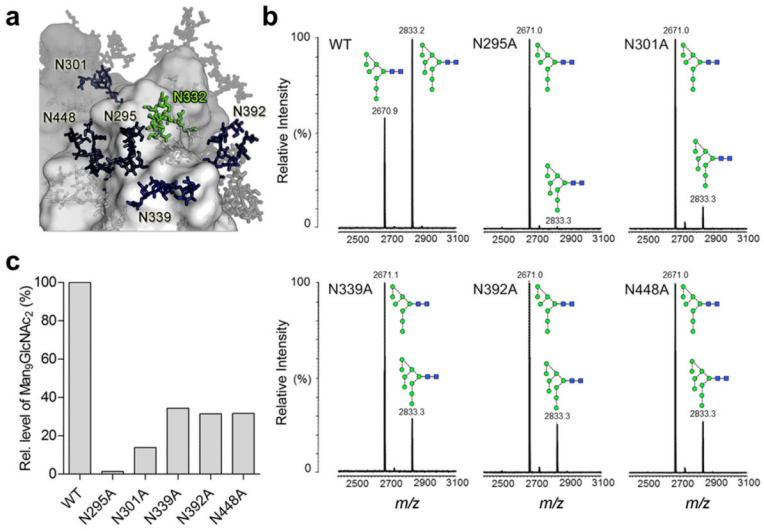

Figure 5. The effect on processing at the N332 glycosylation site by the deletion of neighboring glycans

(**a**) Model of the N332 glycan (green sticks) on the outer domain surrounded by neighboring (dark blue sticks) and distant glycans (gray sticks). (**b**) Site-specific glycan analysis of the N332 site from a panel of mutants lacking the neighboring glycans (Panel A; dark blue glycans). A tryptic glycopeptide containing the N332 site (QAHCNLSR) was isolated and analyzed by MALDI-MS to determine the glycoforms present. The same glycopeptide was analyzed from $gp120_{BaL}$ mutants carrying PNGS-deletions proximal to N332. (**c**) Quantitation of the abundance of $Man_9GlcNAc_2$ on the wild-type and mutant glycopeptides as determined by MALDI-MS. Symbols as in Fig. 2.

Europe PMC Funders Author Manuscripts

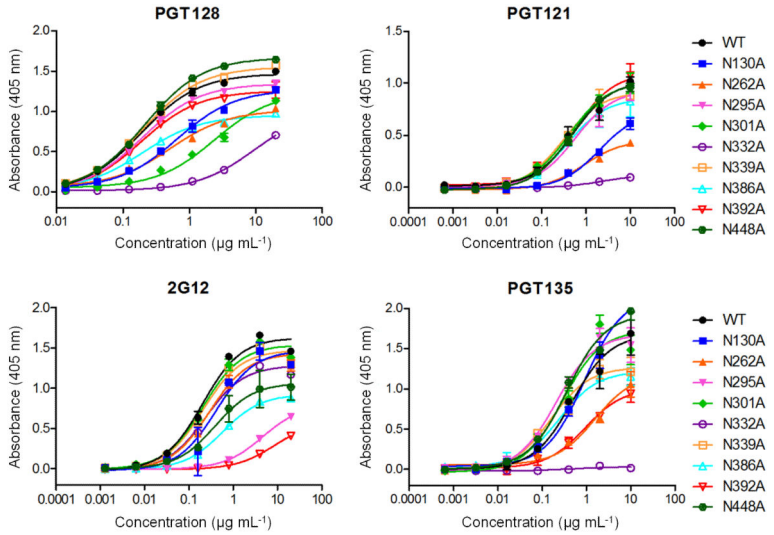

Figure 6. Recognition of glycan site deletion mutants by N332-specific bnAbs

Binding of a panel of N332-specific bnAbs, including 2G12, PGT128, PGT135 and PGT121, was tested against the panel of $gp120_{BaL}$ glycan site deletion mutants by capture ELISA. Error bars represent standard deviation. Each experiment was performed in duplicate and repeated three times.

Europe PMC Funders Author Manuscripts

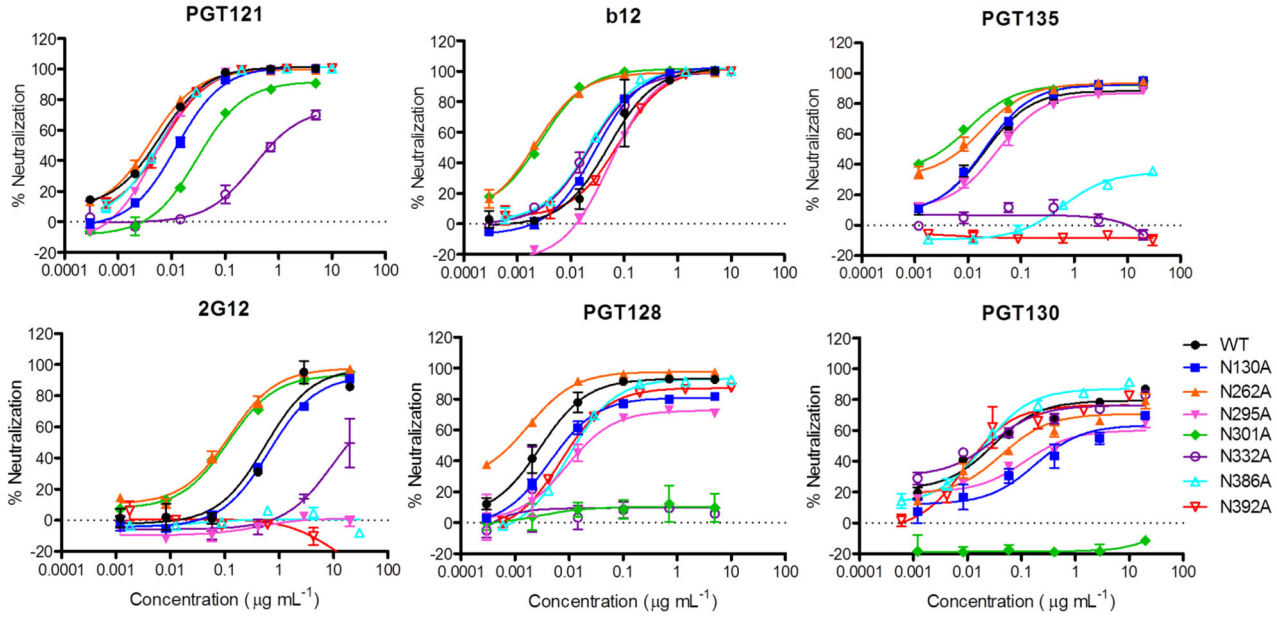

Figure 7. The effect of glycan site deletion on neutralization by N332-specific bnAbs

Neutralization of the BaL wild-type virus and mutant viruses by b12 and N332-specific bnAbs, including PGT121, PGT135, 2G12, PGT128 and PGT130. Error bars represent standard deviation. Each experiment was performed in duplicate and repeated three times.

Europe PMC Funders Author Manuscripts